JOURNAL OF MATERIALS SCIENCE 27 (1992) 175–179

Protonic conduction in $Al_2(SO_4)_3 \cdot 16H_2O$: coulometry, transient ionic current, infrared and electrical conductivity studies

S. A. HASHMI, D. K. RAI, S. CHANDRA
Department of Physics, Banaras Hindu University, Varanasi-221 005, India

Proton transport in $Al_2(SO_4)_3 \cdot 16H_2O$ has been established using different techniques namely coulometry, transient ionic current, i.r., DTA/TGA and electrical conductivity. The possible charge carriers are H^+ and OH^- generated as a result of possible electrolysis of hydrate water molecules. The mobilities of the two charge carriers are approximately 4×10^{-5} and 2.4×10^{-5} $cm^2 V^{-1} s^{-1}$. The electrical conductivity shows strong dependence upon humidity and also shows σ against $1/T$ behaviour closely related with its thermal dehydration reaction.

1. Introduction

Proton conducting solid electrolytes are the materials of special interest due to their many possible applications in various electrochemical devices such as fuel cells/batteries, hydrogen and humidity sensors, electrochromic display devices etc. [1–6]. These materials include many hydrates (e.g. $HUO_2PO_4 \cdot 4H_2O$ [7], $H_3PMo_{12}O_{40} \cdot 29H_2O$ [8], $MoO_3 \cdot 2H_2O$ [9], $(NH_4)_{10}W_{12}O_{42} \cdot 5H_2O$ [10]), some ferroelectric compounds (e.g. ADP [11, 12], KDP [13, 14]), polymeric materials (e.g. PEO–NH_4SCN [15], PEO–NH_4ClO_4 [16], PEO–H_3PO_4 [17]). The present paper reports the proton transport studies on aluminium sulphate hexadecahydrate [$Al_2(SO_4)_3 \cdot 16H_2O$].

The hydrated aluminium sulphate is an important starting material to get fine grained alumina for different applications. The aluminium sulphate hydrate with a very high water content (16 to 17 H_2O) is also known as "Alunogen". The Alunogen has triclinic structure [18] belonging to the space group P1 with $a = 0.7420(6)$ nm; $b = 2.697(2)$ nm; $c = 0.6062(5)$ nm; $\alpha = 89°57(5)'$; $\beta = 97°34(5)'$; $\gamma = 91°53(5)'$; and $z = 2$. The structure is composed of discrete SO_4 and $Al(O_w)_6$ polyhedra interconnected by a network of hydrogen bonds (O_w refers to oxygen of water molecules). Four of the five independent polyhedra are spatially arranged in a manner which gives rise to pseudo-double sheets parallel to (0 1 0). The fifth polyhedron (an SO_4 group) is situated between pseudo-sheets and is surrounded by zeolitic water molecules. Out of 16-hydrates, 12-hydrates are ligand water molecules and rest are zeolitic water. Most of these water molecules can easily come out on heating as evidenced in thermal studies [19, 20].

In the present paper, the proton transport in $Al_2(SO_4)_3 \cdot 16H_2O$ has been established using various experimental techniques namely coulometry, transient ionic current (TIC), i.r. and electrical conductivity. The coulometry followed by gas chromatography suggests the movement of H^+ ions on application of d.c. electrical field. The H^+ ions are generated due to electrolysis of hydrate molecules along with OH^- for transport. σ against $(1/T)$ plot has been explained on the basis of thermal dehydration reaction.

2. Experimental procedure

The transference number was measured on the polycrystalline pellet of $Al_2(SO_4)_3 \cdot 16H_2O$ (pressed at 10 000 kg cm^{-2}) using two methods: (i) polarization, and (ii) direct electrolysis or coulometry [8]. In the polarization technique, the current is monitored as a function of time on applying a constant d.c. voltage across the cell Ag/sample/Ag. This method tells only the total ionic transference number (t_{ion}). The cationic and/or anionic contribution to the "t_{ion}" cannot be identified using this technique. The direct electrolysis or coulometric investigations was carried out to circumvent this problem, using specially designed d.c. electrolysis cell. The details of the electrolysis cell have been reported earlier [8]. The gas evolved (H_2 in the present case) at the cathode side was tested using the gas chromatograph of Tracor Instruments model "540".

The transient ionic current (TIC) measurement technique was used to detect the number of different types of mobile ionic species and to evaluate their mobility. In this method, the sample is first polarised and then the transient ionic current is monitored as a function of time after reversing the polarity of the applied voltage. The mobility, μ, was calculated using the formula

$$\mu = d^2/\tau V \quad (1)$$

where d is thickness of the sample, V is the applied voltage and τ is the time of flight. Details of the experimental technique have been reported elsewhere [21].

0022–2461/92 $03.00 + .12

The i.r. spectra of the electrolysed samples scraped from cathode and anode ends after coulometry along with the original sample were recorded using Perkin-Elmer i.r. spectrophotometer model "883". The spectra were taken in KBr pellets.

The true bulk conductivity was measured from the complex impedance plots with the help of computer controlled Schlumberger Solartron (1250) frequency response analyser coupled with Solartron (1286) Electrochemical Interface. The conductivity was measured in the temperature range 277–388 K.

3. Results and discussion

3.1. Transference number

The total ionic transference number, t_{ion}, has been evaluated using polarization technique and the value of t_{ion} is found to be $\simeq 0.97$. The value of ionic transference number shows that the charge transport is mainly ionic. But, it is difficult to find the cationic and/or anionic contribution to the total ionic transference number using this method. To circumvent this problem, the direct electrolysis has been carried out using a coulometer or d.c. electrolysis cell. The following results have been observed:

(a) On passing a constant current (55.5 μA) through the sample placed in the coulometer, gas evolved both at cathode and anode sides. The volumes of the gases evolved are shown in Fig. 1.

(b) The cathode side gas has been tested using gas chromatography and found to be hydrogen. The gas evolved at the anode and (possibly oxygen and water) is very small and we did not have the facility to detect such a small amount of gas.

(c) The colour of both surfaces of sample was changed after electrolysis. The anode side surfaces became dark black whereas the colour of cathode side surface was feeble brown. The blackening of the anode side surface has been attributed to HgO formation. The coulometer has mercury contacts and escaping O_2 at the anode may result in the formation of HgO. The HgO formation has also been confirmed in i.r. studies (see Section 3.3). We could not assess the charge transfer product at the cathode end but the change in colour may be related to the overall decomposition of the material.

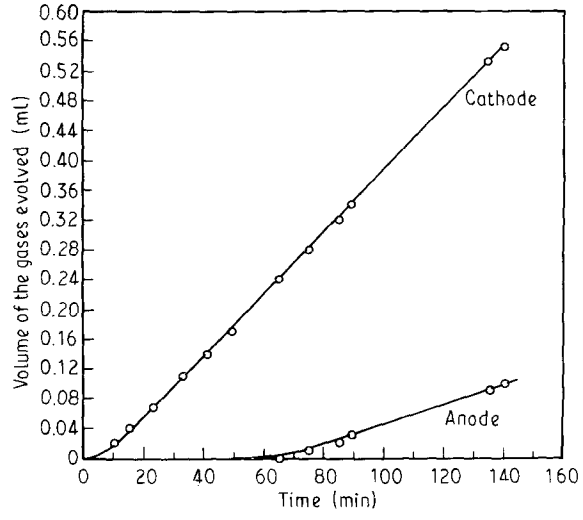

Figure 1 The volume of gases evolved for a constant current (55.5 μA) as a function of time.

The evolution of the gases at both the ends of the coulometer suggests the possible electrolysis of water of crystallization or ligand water and the hydrogen and oxygen evolve as electrolysis products as a result of charge transfer reaction at the electrode-electrolyte interfaces. In $Al_2(SO_4)_3 \cdot 16H_2O$, 12 H_2O molecules are interlayered or ligand water whereas rest of the water molecules are zeolitic hydrates. The ligand water may get electrolysed on application of d.c. electric field following the reaction

$$H_2O \rightarrow H^+ + OH^- \qquad (2)$$

Two types of charge transfer reaction can be considered at the electrode-electrolyte interfaces:

(A) $4H^+ + 4e^- \rightarrow 2H_2$ at cathode

$4\,OH^- \rightarrow 2H_2O + O_2 + 4e^-$ at anode

(B) $4H^+ + 4e^- \rightarrow 2H_2$ at cathode

$4\,OH^- \xrightarrow{-2H_2O} O_2 + 4e^-$ at anode

The Reaction B differs from Reaction A in the sense that in the former H_2O diffuses back in the lattice after liberating O_2 at the anode end whereas in Reaction A it is assumed that H_2O and O_2 are evolved simultaneously. Assuming Reaction B, the transference numbers have been calculated (following Faraday's law of electrolysis) to be $t_{H^+} = 0.88$ and $t_{OH^-} = 0.30$. Total ionic transference number t_{ion} $(t_{H^+} + t_{OH^-}) = 1.18$ exceeds the value 1. This violates the Faraday's law of electrolysis. Following the Reaction A, the transference numbers have been found to be $t_{H^+} = 0.88$ and $t_{OH^-} = 0.1$. The total transference number t_{ion} $(= t_{H^+} + t_{OH^-}) = 0.98$ which agrees approximately with the value of t_{ion} observed from polarization experiment. The reaction mechanism A looks more reasonable.

3.2. Mobility

The TIC measurement technique has been used to detect the number of types of mobile ionic species after electrolysis and to evaluate their mobility. The number of peaks in the transient ionic current against time plot indicates the number of mobile ionic species [21]. Two peaks observed in TIC against time plot (Fig. 2) are indicative of two types of mobile ionic charge carriers (likely species are H^+ and OH^-). The corresponding mobilities have been calculated following the equation (1) and found to be: $\mu_1 = 4 \times 10^{-5}$ and $\mu_2 = 2.4 \times 10^{-5}$ cm^2 V^{-1} s^{-1}. It is difficult to identify the species to which individually these μ_1 and μ_2 are associated with. But, according to relative ionic radii the value of μ_1 and μ_2 may possibly be associated with H^+ and OH^-, respectively.

3.3. I.r. studies

The TIC and coulometric investigations suggest that H^+ and OH^- are transported out as a result of

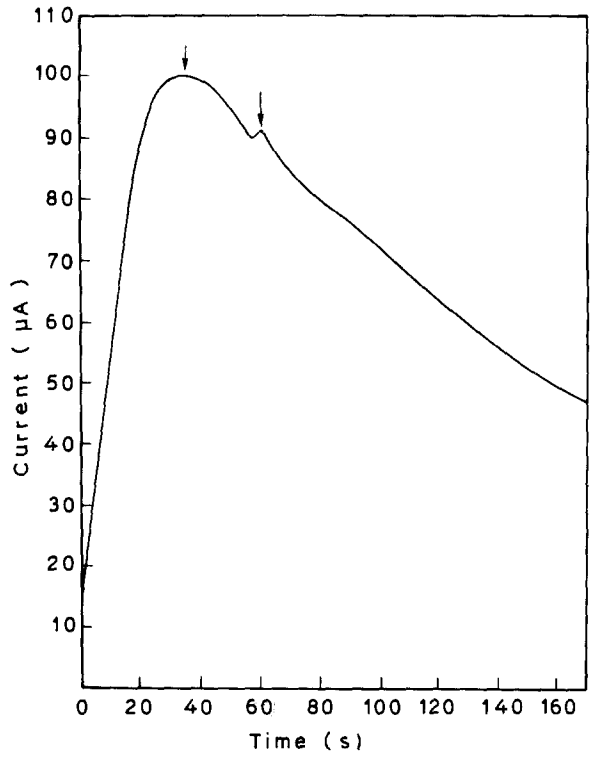

Figure 2 Transient ionic current against time plot.

electrolysis of ligand water. The change in the residual sample after electrolysis has been identified by taking i.r. spectra of the cathode and the anode side samples and comparing it with that of the original sample (Fig. 3). The i.r. spectra of original aluminium sulphate has been studied by Kato and Daimon [20]. Some changes in spectral feature have been observed after electrolysis and are given below:

(i) Two peaks at 1670 and 322 cm^{-1} associated with H–O–H bending and Al–OH twisting, respectively, disappear after electrolysis;
(ii) A peak at 1400 cm^{-1} appear in both the cathode and the anode side samples;
(iii) A peak at 1450 cm^{-1} appears and 575 cm^{-1} peak (related with Al–OH wagging) disappear in cathode side sample only;
(iv) Peaks at 1260, 800 and 475 cm^{-1} appear in anode side sample only; and
(v) A shift of 10 cm^{-1} in a peak at 610 cm^{-1} of ν_4 (SO_4^{2-}) has been observed in the anode side sample.

The disappearance of the peaks at 1670 cm^{-1} associated with H–O–H bending, 322 cm^{-1} associated with Al–OH twisting and 575 cm^{-1} related with Al–OH wagging suggest that the H–O–H species goes out due to the electrolysis of H_2O on application of a d.c. electric field and consequently the absence of Al–OH vibrations in the electrolysed samples has been observed. The observed shift of 10 cm^{-1} in ν_4 band of SO_4^{2-} is as a consequence of H^+ and OH^- evolution after electrolysis which changes the environment of SO_4^{2-}. Some peaks appearing after electrolysis, such as 1400 cm^{-1} band appears in cathode and anode side sample, 1450 cm^{-1} band in cathode side and 1260 cm^{-1} peak in anode side sample which could not be identified by us.

3.4. Electrical conductivity

The bulk electrical conductivity as a function of temperature is shown in Fig. 4 for the temperature range from 277 to 388 K. The true bulk conductivity has

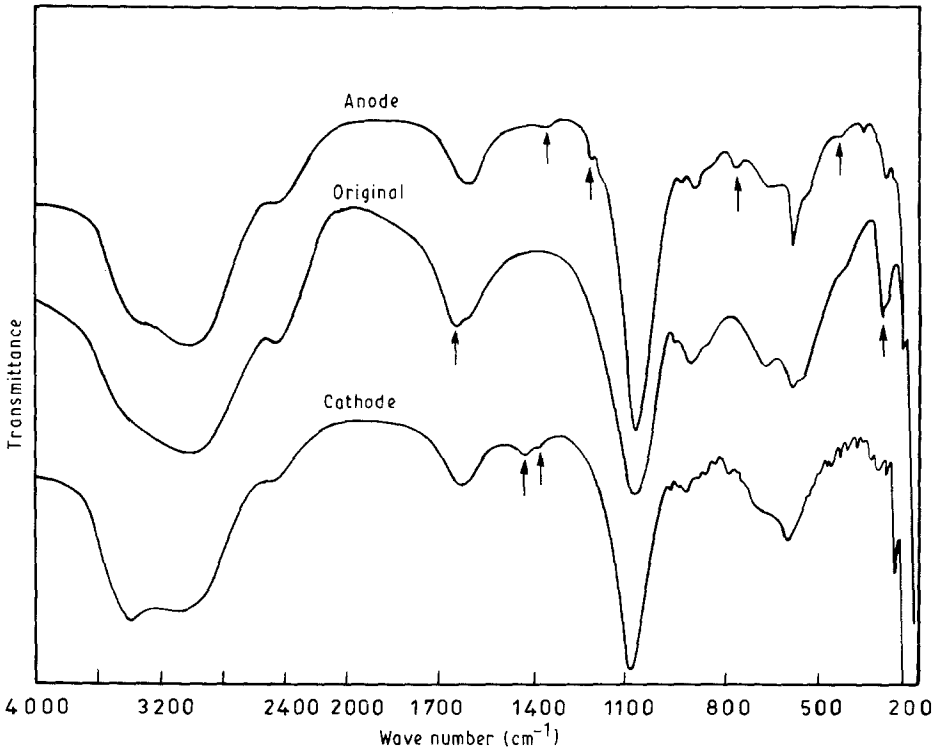

Figure 3 I.r. spectra of original sample and electrolysed sample near cathode and anode.

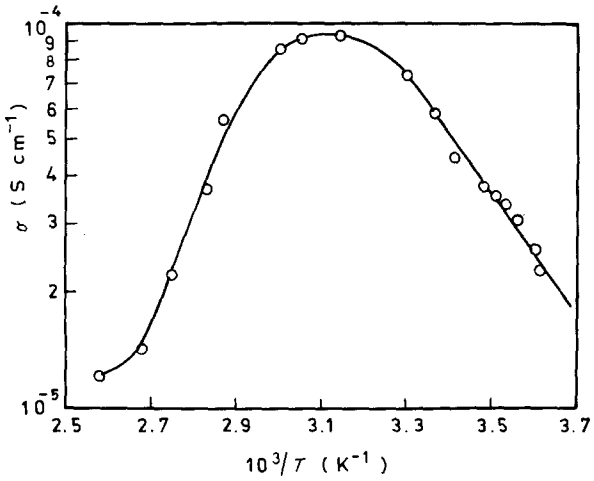

Figure 4 The bulk conductivity as a function of temperature.

been evaluated from experimental complex impedance plots. The conductivity increases initially with increasing temperature upto 323 K showing a linear variation in σ against $1/T$ plot (Fig. 4). This suggests an Arrhenius type thermally activated process for the temperature range from 277 to 323 K. The conductivity can be expressed as

$$\sigma = 10.15 \exp [-0.31(\text{eV})/kT] \quad (3)$$

After the temperature 323 K, the conductivity starts decreasing on further increasing the temperature due to dehydration of $Al_2(SO_4)_3 \cdot 16H_2O$. The onset of dehydration after $\sim$ 323 K is clearly evident in the TGA/DTA record shown in Fig. 5.

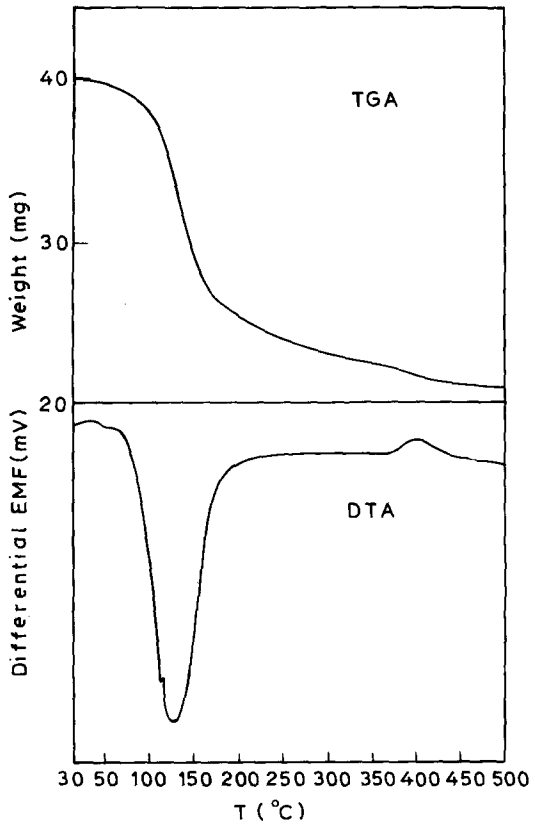

Figure 5 TGA and DTA curve of $Al_2(SO_4)_3 \cdot 16H_2O$.

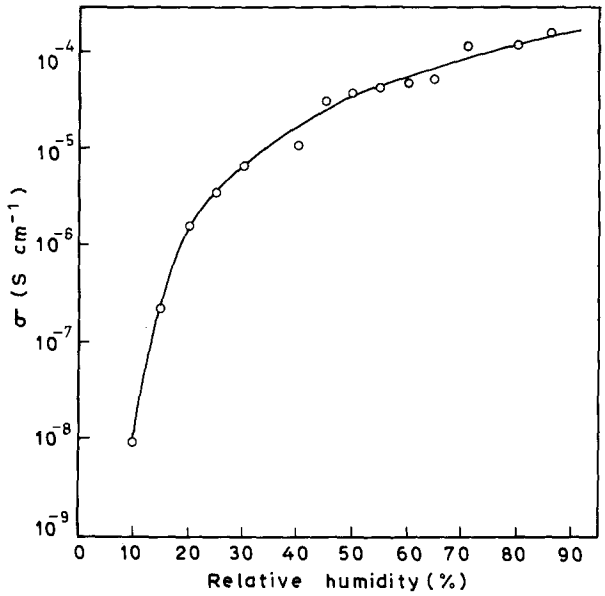

Figure 6 Humidity dependence of the conductivity.

$Al_2(SO_4)_3 \cdot 16H_2O$ is a material in which the H_2O molecules (particularly the zeolitic water) can easily go in and come out of the lattice depending upon the humidity level [18]. This suggests that this material should show a strong humidity dependence. The σ Vs Relative Humidity plot is given in Fig. 6. The σ changes by nearly 10^4 times when r.h. changes from 10 to 86%. However, most of this change is in the region 10 to 40% above which σ changes relatively slowly. This suggests that most of zeolitic water is able to enter the lattice by the time r.h. is 40%. Further, it may be remarked that for r.h. > 86% the pellets started clipping off due to excessive hydration.

4. Conclusion

$Al_2(SO_4)_3 \cdot 16H_2O$ is a proton conductor with H^+ and OH^- charge carriers ($t_{H^+} = 0.88$, $t_{OH^-} = 0.1$). The ligand water present in $Al_2(SO_4)_3 \cdot 16H_2O$ provides the charge carriers H^+ and OH^-. I.r. studies confirm the above hypothesis of electrolysis. The conductivity is humidity and temperature dependent. The temperature dependence of electrical conductivity has been explained on the basis of Arrhenius type thermally activated process upto 323 K beyond which the conductivity decreases due to dehydration.

Acknowledgement

We are grateful to DNES (New Delhi) for the financial support to complete this work. Our thanks are also due to Dr A. K. Kashyap, Dr S. P. Singh and Dr K. D. Pandey of the Botany Department, Banaras Hindu University, for providing the gas chromatographic facility.

References

1. J. JENSEN and M. KLEITZ, "Solid State Protonic Conductors I" (Odense University Press, Denmark, 1981).
2. J. B. GOODENOUGH, J. JENSEN and M. KLEITZ, "Solid

State Protonic Conductors II" (Odense University Press, Denmark, 1982).
3. *Idem.*, "Solid State Protonic Conductors III" (Odense University Press, Denmark, 1985).
4. R. C. T. SLADE, "Solid State Protonic Conductors IV" (North Holland, Amsterdam, 1988).
5. S. CHANDRA, N. SINGH and S. A. HASHMI, *Proc. Ind. Natl. Sci. Acad.* **52** (1986) 338.
6. S. CHANDRA, *Materials Science Forum* **1** (1984) 153.
7. A. T. HOWE and M. G. SHILTON, *J. Solid State Chem.* **28** (1979) 345.
8. O. NAKAMURA, T. KODAMA, I. OGINO and Y. MIYAKE, *Chem. Lett.* **17** (1979).
9. S. CHANDRA, B. SINGH and N. SINGH, *Solid State Comm.* **57** (1986) 519.
10. S. CHANDRA, S. K. TOLPADI and S. A. HASHMI, *J. Phys.: Condens. Matter* **1** (1989) 9101.
11. S. CHANDRA and S. A. HASHMI, *J. Mater. Sci.* **25** (1990) 2459.
12. E. J. MURPHY, *J. Appl. Phys.* **35** (1964) 2609.
13. L. B. HARRIS and G. L. VELA, *J. Chem. Phys.* **58** (1973) 4550.
14. S. CHANDRA and AJAY KUMAR, *Solid State Ionics* **40/41** (1990) 863.
15. M. STAINER, L. C. HARDY, D. H. WHITMORE and D. F. SHRIVER, *J. Electrochem. Soc.* **131** (1984) 784.
16. S. A. HASHMI, AJAY KUMAR, K. K. MAURYA and S. CHANDRA, *J. Phys. D: Appl. Phys.* (1990) 1307.
17. P. DONOSO, W. GORECKI, C. BERTHIER, F. DEFENDINI, C. POINSIGNON and M. B. ARMAND, *Solid State Ionics* **28–30** (1988) 969.
18. J. H. FANG and P. D. ROBINSON, *Amer. Mineral.* **61** (1976) 311.
19. T. SATO, F. OZAWA and S. IKOMA, *J. Appl. Chem. Biotechnol.* **28** (1978) 811.
20. E. KATO and K. DAIMON, *J. Amer. Ceram. Soc.* **62** (1979) 313.
21. S. CHANDRA, S. K. TOLPADI and S. A. HASHMI, *Solid State Ionics* **28–30** (1988) 651.

Received 21 August 1990
and accepted 31 January 1991